

# AFM Study of Two-Dimensional Epitaxial Arrays of Poly( $\gamma$ -L-glutamates) with Long $n$ -Alkyl Side Chains on Graphite

Tatsuya Imase,<sup>†</sup> Akihiro Ohira,<sup>†</sup> Kento Okoshi,<sup>‡,§</sup> Naoko Sano,<sup>†</sup> Susumu Kawauchi,<sup>‡,§</sup> Junji Watanabe,<sup>\*,‡,§</sup> and Masashi Kunitake<sup>\*,†</sup>

Department of Applied Chemistry & Biochemistry, Faculty of Engineering, Kumamoto University, 2-39-1 Kurokami, Kumamoto 860-8555, Japan; Department of Organic and Polymeric Materials, Tokyo Institute of Technology, 2-12-1 O-okayama, Meguro-ku, Tokyo 152-0033, Japan; and CREST-JST (Japan Science and Technology Corporation), 4-1-8 Hon-cho, Kawaguchi, Saitama 332-0012, Japan

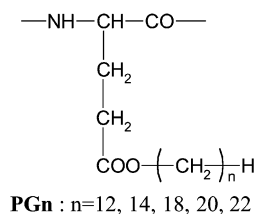
Received September 3, 2002; Revised Manuscript Received December 28, 2002

**ABSTRACT:** Two-dimensional (2D) arrays of poly( $\gamma$ - $n$ -alkyl L-glutamates) (**PGn**) on HOPG are found to be formed by casting under conditions producing submonolayer coverage. Direct observation of the arrays in a series of polymers using atomic force microscopy allowed clear visualization of the island structures, which consisted of parallel running rods. The helical polymer chains were epitaxially aligned to form rods with a "head to head" or a "head to tail" association. In the array composed of rods, the extended alkyl side chains with all-trans conformation are divided to both sides of a helical main chain and align perpendicularly to the main chain. The interval distances between parallel rods in the island increased linearly by about 2.2 Å/CH<sub>2</sub> unit with increasing alkyl side chain length. Epitaxial adsorption of alkyl chain moieties onto graphite is the primary driving force in the formation of the 2D array structure of these helical polymers.

## 1. Introduction

The micro- and/or mesoscopic structures of polymers adsorbed on substrates are of considerable interest both for advancing fundamental understanding and for developing potential applications. The scanning probe microscope techniques (SPM), such as scanning tunnel microscopy (STM) and atomic force microscopy (AFM), provide the opportunity for direct observation or visualization of polymers on atomic flat substrates with submolecular resolution. Observations of biopolymers, such as DNA<sup>1–4</sup> and synthetic polymers<sup>5–8</sup> in the isolated or aggregated state using SPM, mainly AFM, have been conducted in order to analyze molecular characteristics such as chain length, end-to-end length, polymer diameters, chain rigidity, and so on.<sup>9–11</sup> The adsorption of various molecules with alkyl long chains, including polymers, onto highly oriented pyrolytic graphite (HOPG) has also been reported,<sup>12–16</sup> permitting the formation of epitaxial adlayers and relatively easy visualization by STM. Such epitaxial adlayers of oligomer and polymers on HOPG have also been prepared by adsorption from phenyl-octane solution<sup>17</sup> and epitaxy-induced polymerization.<sup>18</sup>

Here, we report the AFM visualization of poly( $\gamma$ -L-glutamate) derivatives with a series of alkyl long chains adsorbed on HOPG. These polymers are characterized by the following general structure



where  $n$  is defined here as the number of methylene units of the alkyl group.

Poly( $\gamma$ -L-glutamates) are well-known to form a stable  $\alpha$ -helical conformation even when the substituted side chains are varied. Studies of the crystal structure of poly( $\gamma$ -L-glutamate) derivatives have focused primarily on the packing structure of the  $\alpha$ -helices. Kaufman et al.<sup>19</sup> initially reported that long  $n$ -alkyl side chains of polymers based on acrylic and methacrylic acids can pack into paraffin-like crystallites. Watanabe et al.<sup>20</sup> discovered the thermotropic liquid crystal nature of these polymers and investigated the molecular packing and thermotropic behaviors for a series of poly( $\gamma$ -L-glutamates) with  $n$ -alkyl side chains changing from amyl to octadecyl.

The present study involved not only the visualization of polypeptides by AFM but also a comparison between the local structures in 3D bulk crystal and the adlayer structure in terms of alkyl side chains packing.

## 2. Experimental Section

**2.1. Materials.** A series of poly( $\gamma$ - $n$ -alkyl L-glutamates) (**PGn**) were synthesized by the conventional NCA method.<sup>21,22</sup> All the polymers are designated by the letter **PG** followed by the number of carbons in the side chain alkyl group  $n$ . The averaged molecular weights were estimated to be  $M_w = 113\,300$  and polydispersity index ( $M_w/M_n$ ) = 1.69 for **PG12**;

<sup>†</sup> Kumamoto University

<sup>‡</sup> Tokyo Institute of Technology

<sup>§</sup> CREST-JST.

\* Corresponding authors: e-mail kunitake@chem.kumamoto-u.ac.jp and jwatanab@polymer.titech.ac.jp.

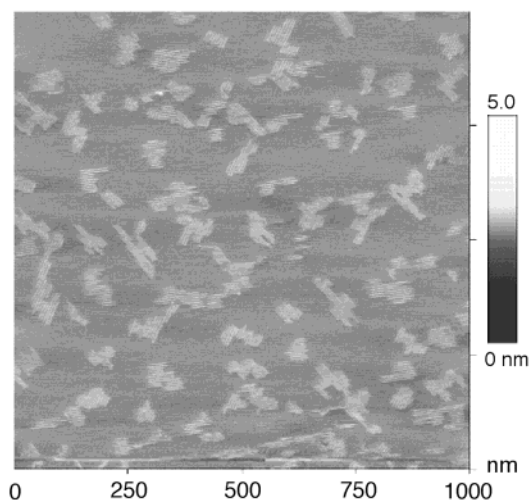


**Figure 1.** A typical AFM image of **PG18B** adlayers on HOPG substrate with submonolayer coverage prepared by the casting of chloroform solutions ( $2\ \mu\text{mol unit}$ ).

$M_w = 30\ 200$  and  $M_w/M_n = 1.23$  for **PG14**;  $M_w = 57\ 700$  and  $M_w/M_n = 4.58$  for **PG20**; and  $M_w = 60\ 150$  and  $M_w/M_n = 1.49$  for **PG22** by a GPC analysis (THF, 300 K) using calibration with polystyrene standards. To investigate the effect of molecular weight, we prepared two **PG18s** ( $M_w = 37\ 914$ , with  $M_w/M_n = 1.1$  for **PG18A** and  $M_w = 56\ 059$  and  $M_w/M_n = 1.2$  for **PG18B**). The chloroform solvent was obtained from Sigma-Aldrich Chem. Co., Inc.

**2.2. Measurements.** Polypeptides were dissolved at concentrations of approximately  $2\ \mu\text{mol}$  of ( $\gamma$ -*n*-alkyl L-glutamates unit)/L in chloroform. All solutions were kept at room temperature. Polypeptides were cast on a freshly cleaved, basal plane of highly oriented pyrolytic graphite (HOPG, grade STM-1, Advanced Ceramics Co., Lakewood, OH) using a solution volume of  $3\text{--}5\ \mu\text{L}$ . The samples were subsequently dried at room temperature in air. All AFM images were obtained in air and at room temperature using an AFM (NanoScope IIIa, Digital Instruments, Santa Barbara, CA) operated by tapping mode (registered name, Digital Instruments). Silicon tips were purchased from the same manufacturer. All the AFM images presented here were flattened using software, but no other digital operation was carried out.

### 3. Results and Discussion

The casting of small amounts of very dilute chloroform solution ( $2\ \mu\text{mol unit}$ ) allows formation of molecular layers with submonolayer coverage. Under such conditions, the polymer solution forms two-dimensional (2D) arrays of **PGn** with *n*-alkyl side chains on HOPG. To investigate the effect of alkyl chain length, a series of polymers (**PG12**, **PG14**, **PG18**, **PG20**, and **PG22**) were prepared as submonolayer films on HOPG, and the morphologies of the polymers were investigated by AFM.

In whole polymer systems, adsorbed polymers were visualized as a scattered islandlike feature in AFM images. Similar AFM images of islandlike featured dendritic polymers with alkyl chains on HOPG have been reported from Percec and co-workers.<sup>8</sup> As a typical example, Figure 1 shows an AFM image of the **PG18A** adlayer with a relatively wide view area. In the image, the entire surface is uniformly covered by bright islands, representing the polymer adsorbates, and the dark portion surrounding islands is bare graphite surface. The constant contrast for island features indicated that the islands consisted of flat monolayers, not multilayers. In addition, the shape of islands seemed to be rectangular, not circular.

Interestingly, high-resolution images revealed the island structures to have strips. Figure 2 shows the collection of island images for the **PGn** series. The islandlike arrays consisted of rods, which possessed an entirely straight conformation in a parallel arrangement. All images except those of **PG12** revealed a similar island structure. For **PG12**, the island images were obscured, and the striped pattern could not be seen (Figure 3). In images of all polymers, the islands consisted of at least three rods. A single rod, which was separated from the islands, was not found at all. The corrugations of the islands were regularly in size at approximately  $0.25 \pm 0.2\ \text{nm}$ , and there seemed to be no essential differences between the polymer samples with the exception of differences attributable to error. Cross-section profiles of the island structures are shown in the insets of the images. The corrugations of the islands observed by AFM were smaller than height expected for PG polymers, even for PMLG. It is well-known that the corrugations in AFM images might not represent the actual height of adsorbates, because the force balances between the adsorbate and the AFM tip are different than those between the substrate and the tip. However, it is important to emphasize that the corrugations of the islands were constant for every **PGn** series. This would suggest that the alkyl chains on PG polymers lay flat and touch graphite in the same manner. It also indicates that the polymers adsorbed on HOPG not in an aggregated form, but in a monolayer form.

In Figure 2c,g, the marked arrows indicate the running direction of the stripes in the islands. The striped patterns in the arrays are triangular in arrangement with the direction of the running stripes rotated  $60^\circ$  from each other, attributed to the  $\langle 1\bar{2}10 \rangle$  direction. This clearly indicates that the formation of the island structures is by epitaxial adsorption.

The interval distances between the parallel rods depended on the length of the alkyl side chains of the polymers. Figure 4 shows plots of the intervals between the parallel rods against the number of alkyl side chains. The intervals increased linearly with the length of the alkyl side chains. From the slope of the linear plot, the length per methylene unit is about  $2.2\ \text{\AA}$ , which corresponds to the overall increment of an extended alkyl chain with an all-trans conformation. It indicates that the alkyl side chains perpendicular to a helical main chain. The extrapolated value of the interval to  $n = 1$  which should correspond to the interval for poly-( $\gamma$ -L-glutamates) (PMLG,  $n = 1$ ) was  $19.9\ \text{\AA}$ . This value is appropriate as the diameter of PMLG, which validates the model subsequently proposed.

All results suggest an epitaxial model of adsorption and self-organization of polymers on HOPG in the **PGn** series. Figure 5a shows the schematic representation of the structural model proposed for **PG**. In the array model, the intervals of rods correspond to intermolecular distances between flat oriented adjacent polymers. Extended alkyl side chains with the all-trans conformation would be divided to both sides of a helical main chain and align toward the directions perpendicular to the main chain. The driving force for the formation of the array is dominantly an epitaxial interaction between the alkyl side chains and the graphite surface. The arrangement of alkyl chains of **PGn** followed the normal epitaxial arrangement of alkane on the graphite basal plan. As mentioned before, the rods of **PGn** run

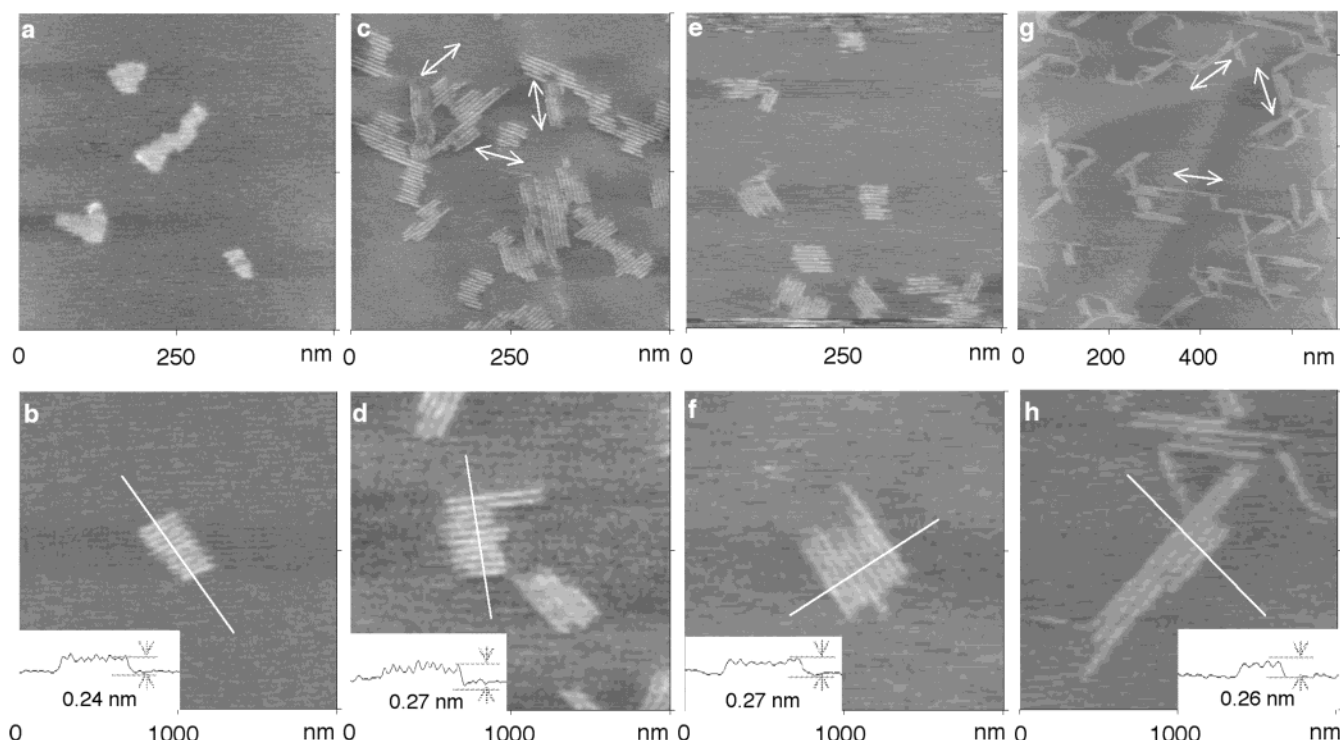


**Figure 2.** AFM images and cross-sectional profiles (insets) of **PG $n$**  adsorbed on HOPG substrate: (a, b) **PG14**, (c, d) **PG18A**, (e, f) **PG18B**, and (g, h) **PG22**. The Z-scale of the images is constant at 4 nm. The arrows indicated the running directions of the rods in the 2D array, and the directions corresponded to  $\langle 12\bar{1}0 \rangle$  directions of the graphite basal plane.

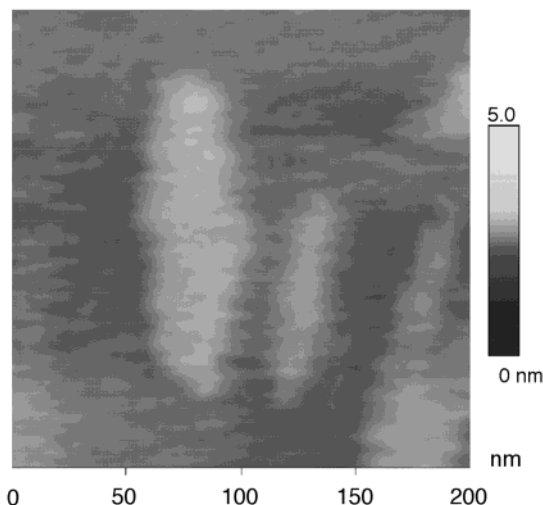


**Figure 3.** AFM image of **PG12** adsorbed on HOPG substrate. The Z-scale of the images is constant at 4 nm.

in the  $\langle 12\bar{1}0 \rangle$  direction. When the rod model was superimposed on a graphite lattice, the alkyl side chains, which were angled at  $90^\circ$  to the direction of the rods, were aligned in the  $\langle 10\bar{1}0 \rangle$  direction. It is well-known that alkyl chains epitaxially adsorb on HOPG and that alkyl chains are aligned in the  $\langle 10\bar{1}0 \rangle$  direction. This fact clearly proves the accuracy of the proposed model and indicates that the formation of the array is dominantly due to epitaxial adsorption of the side groups. The adsorption stability of the alkanes increases with increasing chain length. Although the interactions between the alkanes and the graphite are stronger than intermolecular interactions,<sup>16b</sup> the lateral intermolecular interactions are an important in the formation of an ordered 2D structure. As mentioned above, the primary driving force for the formation of the epitaxial

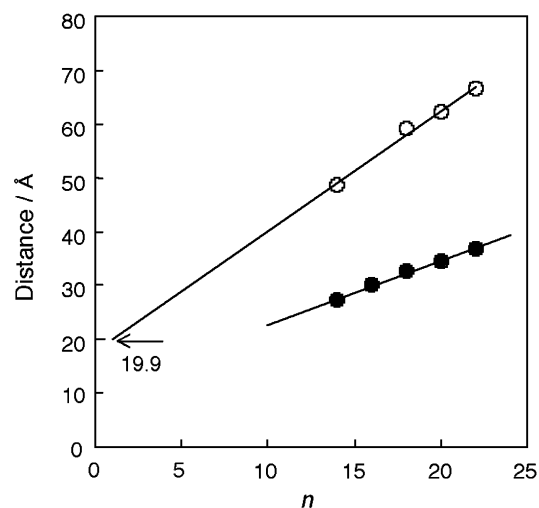


**Figure 4.** Variations in interval distances (open circles) between neighboring rods in the 2D array and the corresponding distances (closed circles) between the center of the polypeptides in bulk crystal, which is revealed as the (100) reflections.

adlayer is the epitaxial interaction between the alkyl side chains and the graphite surface. However, the formation of island structure composed of rods suggests the existence of the attractive intermolecular interaction between the alkyl chains of adjacent rods, involving such interactions as van der Waals forces.

Alkyl chains have also been reported to align "side by side" with parallel or perpendicular conformations at the surface.<sup>12a,16b</sup> In the case of the **PG $n$**  series, the expected interval between alkyl chains is 0.30 nm, which is just twice the length of each  $\alpha$ -helix per residue (0.15 nm), because the alkyl chains divided to left and right sides of the helix. The interval between the alkyl



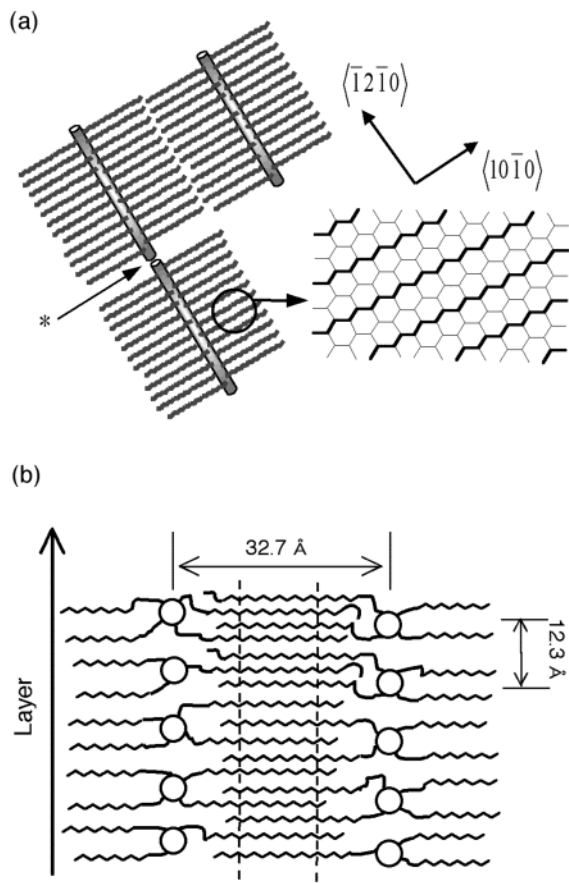


**Figure 5.** Schematic representation of the proposed structural models for the 2D array showing the rod structure and the epitaxial alignment of alkyl side chains on HOPG substrate (a) and for the bulk crystal viewed parallel to the chain axes of the  $\alpha$ -helices (b) of the **PG $n$**  series.

chains is very close to that reported for a flat conformation.

From the model, it was expected that the length of the rods was attributable to the length of each helical polymer. However, the lengths of strings observed were regularly several times longer than expected. For examples, the observed length of rods for **PG18A** ( $M_w = 37\,914$ ,  $M_w/M_n = 1.1$ ; expected length = 15 nm) and **PG18B** ( $M_w = 56\,059$ ;  $M_w/M_n = 1.2$ ; expected length = 22 nm) were 27–44 and 17–98 nm, respectively. This observation would indicate that each rod consisted of several polymers to form “head to head” or “head to tail” structures indicated by the arrow in Figure 5a. The reason for such an interpolymer arrangement “side by side” would be intermolecular interactions between the alkyl chains of adjacent rods. Furthermore, the rods of **PG22** (Figure 2g) were longer than those of other **PG $n$** s, although the average degree of polymerization for **PG22** was almost the same as that of **PG18B** (Figure 2e). This observation is not due to differences in the molecular weights of the polymers, but probably due to the enhancement of intermolecular interactions with the increments of alkyl chain length. Moreover, the rods seem to have a tendency to align the edges of rods. The islands in Figure 2b,d,f are typical examples with relatively ordered rod ends. This suggests attractive lateral intermolecular interactions between rods at the surface. In addition, when the samples were heated to 110 °C (decomposition temperature >200 °C) and cooled slowly, the island structure consisting of the rods was

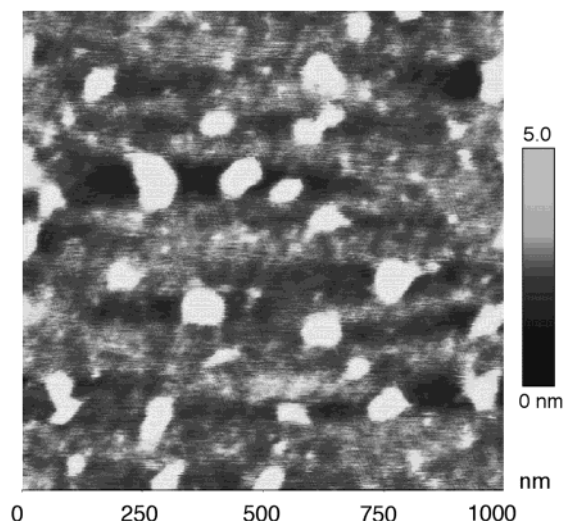


**Figure 6.** Typical AFM images of **PG18B** films on HOPG substrate prepared by casting (2  $\mu$ mol unit, 0.3 mL per about 0.2 cm<sup>2</sup>) after thermal treatment (heating at 100 °C and slow cooling).

preserved and the islands became larger. The growth of the islands also indicates that the island formation is due to a self-organizing process caused by intermolecular interactions.

A comparison between the crystal structures of the 2D array and the bulk state of **PG $n$**  would be potentially interesting. Figure 5b shows a schematic representation of the structural model in the bulk crystal.<sup>20b</sup> The bulk crystal for polypeptides of  $n \geq 10$  has a lamella-like crystal structure (Figure 5b), in which the side chains were divided to both sides the same as the epitaxial structure on HOPG and crystallized in a similar manner as alkane crystals. However, in the bulk crystals, the alkyl side chains of adjacent rods are interdigitated with each other, whereas those of the 2D array are not. In fact, this difference was revealed in the plots of intervals against alkyl length ( $n$ ). In Figure 4, the results of bulk crystal analysis are plotted with those of the 2D array. The slope for the **PG $n$**  bulk crystal, in which the side chains were crystallized, was approximately 1.3 Å/CH<sub>2</sub> (a methylene unit), which is almost half the value of that for the 2D crystal. This difference is due to the interdigitating structure of the bulk crystal.

Macroscopically low coverage of the polymer adlayers was utilized in order to investigate the adsorption of polymers at the submolecular level. As mentioned above, the appearance of 2D arrays rather than 3D crystals indicates that the polymer–surface interactions overcome the intermolecular interactions that tend to form a bulk crystal structure. This proposed structure is also supported by the thermal treatments results, as mentioned above. The observation of adlayers with a relatively high coverage revealed the relation between the 2D array and the bulk crystal.

The surface morphology in the case of films that are thicker but close to monolayer thickness is drastically different from that of submonolayer coverage (Figure 1). As a typical example, Figure 6 shows the AFM image of the **PG18B** cast film which exceeds the thickness of a monolayer. The surface of the cast film showed a lot of hemispheric protrusions several tens of nanometers in size, which was caused by 3D aggregation of the polymer. Moreover, the regular monolayer arrangements formed by parallel rods, which corresponded to

the island structure, were also observed in the flat portions surrounding the protrusions. The thermal treatment did not influence the morphology of coexisting epitaxial monolayer and hemispheric protrusions. The coexistence of 3D crystal and 2D array structures indicates that the polymer adsorbed on the epitaxial monolayer tend to form 3D aggregates, possessing an essentially similar structure to that of the bulk crystal, rather than "layer by layer" structure based on the 2D array structure.

#### 4. Conclusion

A two-dimensional (2D) array of poly( $\gamma$ -*n*-alkyl L-glutamates) (**PGn**) on HOPG is found to form under submonolayer coverage conditions. Despite the relatively low resolution of the AFM compared to the STM, all results including the correlation between the interval of rods and alkyl chain lengths clearly proved the proposed model for epitaxial adsorption of **PGn**. These results are significant in furthering understanding of liquid crystal behaviors and the bulk structure of helical polymers.

**Acknowledgment.** This research was supported by CREST-JST and a Grant-in Aid for Scientific Research from the Ministry of Education, Science, Sports and Culture.

#### References and Notes

- (1) Kanno, T.; Tanaka, H.; Miyoshi, N.; Kawai, T. *Appl. Phys. Lett.* **2000**, *77*, 3848–3850.
- (2) Hamai, C.; Tanaka, H.; Kawai, T. *J. Phys. Chem. B* **2000**, *104*, 9894–9897.
- (3) Hansma, H. G. *Annu. Rev. Phys. Chem.* **2001**, *52*, 71–92.
- (4) Sanches-Sevilla, A.; Thimonier, J.; Marilley, M.; Rocca-Serra, J.; Barbet, J. *Ultramicroscopy*, in press.
- (5) Ohnishi, S.; Hara, M.; Furuno, T.; Sasabe, H. *Jpn. J. Appl. Phys.* **1996**, *35*, 6233–6238.
- (6) Furuno, T. *Jpn. J. Appl. Phys.* **2000**, *39*, 6435–6440.
- (7) (a) Idiris, A.; Alam, M. T.; Ikai, A. *Protein Eng.* **2000**, *13*, 763–770. (b) Jandt, K. D.; Finke, M.; Cacciafesta, P. *Colloids Surf. B* **2000**, *19*, 301–314.
- (8) (a) Percec, P.; Ahn, C.-H.; Ungar, G.; Yeardley, D. J. P.; Moeller, M.; Sheiko, S. S. *Nature (London)* **1998**, *391*, 161–164. (b) Percec, V.; Holerca, M. N.; Magonov, S. N.; Yeardley, D. J. P.; Ungar, G.; Duan, H.; Hudson, S. D. *Biomacromolecules* **2001**, *2*, 706–728.
- (9) (a) Kumaki, J.; Nishikawa, Y.; Hashimoto, T. *J. Am. Chem. Soc.* **1996**, *118*, 3321–3322. (b) Ebihara, K.; Koshihara, S.; Yoshimoto, M.; Maeda, T.; Ohnishi, T.; Koinuma, H.; Fujiki, M. *Jpn. J. Appl. Phys.* **1997**, *36*, L1211–L1213.
- (10) Balnois, E.; Stoll, S.; Wilkinson, K. J.; Buffle, J.; Rinaudo, M.; Milas, M. *Macromolecules* **2000**, *33*, 7440–7447.
- (11) Camesano, T. A.; Wilkinson, K. J. *Biomacromolecules* **2001**, *2*, 1184–1191.
- (12) (a) Rabe, J. P.; Buchholz, S. *Science* **1991**, *253*, 424–427. (b) Hentschke, R.; Shurmann, B. L.; Rabe, J. P. *J. Chem. Phys.* **1992**, *96*, 6213–6221.
- (13) Hentschke, R.; Winkler, R. G. *J. Chem. Phys.* **1993**, *99*, 5528–5534.
- (14) (a) Claypool, C. L.; Faglioni, F.; Goddard, W. A., III; Gray, H. B.; Lewis, N. S.; Marcus, R. A. *J. Phys. Chem. B* **1997**, *101*, 5978–5995. (b) Faglioni, F.; Christopher, C. L.; Lewis, N. S.; Goddard, W. A., III *J. Phys. Chem. B* **1997**, *101*, 5996–6020.
- (15) (a) Rabe, J. P.; Buchholz, S.; Askadskaya, L. *Synth. Met.* **1993**, *54*, 339–349. (b) Stabel, A.; Rabe, J. P. *Synth. Met.* **1994**, *67*, 47–53. (c) Stabel, A.; Herwig, P.; Müllen, K.; Rabe, J. P. *Angew. Chem., Int. Ed. Engl.* **1995**, *34*, 1609–1611.
- (16) (a) Qui, X.; Wang, C.; Zeng, Q.; Xu, B.; Yin, S.; Wang, H.; Xu, S.; Bai, C. *J. Am. Chem. Soc.* **2000**, *122*, 5550–5556. (b) Yin, S.; Wang, C.; Qiu, X.; Xu, B.; Bai, C. *Surf. Interface Anal.* **2001**, *32*, 248–252.
- (17) Stecher, R.; Gompf, B.; Münter, J. S. R.; Effenberger, F. *Adv. Mater.* **1999**, *11*, 927–931.
- (18) (a) Sano, M.; Sasaki, D. Y.; Kunitake, T. *J. Chem. Soc., Chem. Commun.* **1992**, *18*, 1326–1327. (b) Sano, M.; Sasaki, D. Y.; Kunitake, T. *Macromolecules* **1992**, *25*, 6961–6969.
- (19) Kaufman, H. S.; Sacher, S.; Alfrey, T.; Frakuchen, I. *J. Am. Chem. Soc.* **1948**, *70*, 3147.
- (20) (a) Watanabe, J.; Fukuda, Y.; Gehani, R.; Uematsu, I. *Macromolecules* **1984**, *17*, 1004–1009. (b) Watanabe, J.; Ono, H.; Uematsu, I.; Abe, A. *Macromolecules* **1985**, *18*, 2141–2148. (c) Watanabe, J.; Ono, H. *Macromolecules* **1986**, *19*, 1079–1083. (d) Watanabe, J.; Goto, M.; Nagase, T. *Macromolecules* **1987**, *20*, 298–304. (e) Watanabe, J.; Nagase, T. *Polym. J.* **1987**, *19*, 781–784. (f) Watanabe, J.; Nagase, T. *Macromolecules* **1987**, *21*, 171–175. (g) Ono, H.; Watanabe, J.; Abe, A. *Kobunshi Ronbunshu* **1988**, *45*, 69–77.
- (21) Smith, J. C.; Woody, R. W. *Biopolymers* **1973**, *12*, 2657.
- (22) Wasserman, D.; Garber, J. D.; Meigs, F. M. U.S. Patent 3 285 953, 1966.

MA021421Z